whose primal parts $A(\psi)$, $B(\psi)$ and $C(\psi)$ are identical to those of the spherical linkage, as displayed in eqs.(3.88b), their dual parts $A_o(\psi)$, $B_o(\psi)$ and $C_o(\psi)$ being obtained with the aid of computer algebra and the rules of operations with dual numbers, namely,

$$\begin{aligned} A_o &= k_{3o}c\psi - k_3 d_2 s\psi - k_{4o} && (3.91a)\\ B_o &= s\psi + d_2 c\psi && (3.91b)\\ C_o &= k_{1o} + k_{2o}c\psi - k_2 d_2 s\psi && (3.91c) \end{aligned}$$

in which the Freudenstein parameters are now dual numbers: $\hat{k}_i = k_i + \epsilon k_{io}$, for $i = 1, \ldots, 4$. Moreover, their primal part is identical to that of the spherical four-bar linkages, their dual parts being displayed in eqs.(3.42) and reproduced below for quick reference.

$$\begin{aligned} k_{o1} &= -\frac{a_1\lambda_2\lambda_4\mu_1\mu_2\mu_4 + a_2(\lambda_1\lambda_4 - \lambda_2\lambda_3)\mu_4 - a_3\mu_2\mu_3\mu_4 + a_4(\lambda_1\lambda_2 - \lambda_3\lambda_4)\mu_2}{\mu_2^2\mu_4^2}\\ k_{o2} &= \frac{a_1\lambda_1\lambda_4\mu_4 - a_4\mu_1}{\mu_4^2}, \quad k_{o3} = -a_1\mu_1, \quad k_{o4} = \frac{a_1\lambda_1\lambda_2\mu_2 - a_2\mu_1}{\mu_2^2} \end{aligned}$$

Once we have obtained the input-output equation in terms of dual angles, it is possible to analyze the RCCC linkage, which allows us, in turn, to compute all the joint rotations and translations. The input-output equation above can be generally written as

$$\hat{\mathcal{L}}: \quad \hat{A}\hat{u} + \hat{B}\hat{v} + \hat{C} = 0 \tag{3.92a}$$

and

$$\hat{\mathcal{C}}: \quad \hat{u}^2 + \hat{v}^2 = 1 \tag{3.92b}$$

where

$$\hat{u} = \cos\hat{\phi}, \quad \hat{v} = \sin\hat{\phi} \tag{3.92c}$$

Equations (3.92a–c) represent a *dual line* $\hat{\mathcal{L}}$ and a *dual unit circle* $\hat{\mathcal{C}}$ in the dual $\hat{u}$-$\hat{v}$ plane, respectively. Now, it is possible to decompose the equation of the "line" $\hat{\mathcal{L}}$ into two real equations, one for its primal, and one for its dual part, namely,

$$\mathcal{P}: \quad Au + Bv + C = 0 \tag{3.93a}$$

$$\mathcal{H}: \quad (A_o + Bd_1)u - Ad_1v + C_o = 0 \tag{3.93b}$$

For the circle $\hat{\mathcal{C}}$, the dual part vanishes identically, the primal part leading to a *real circle*, namely,

$$\mathcal{C}: \quad u^2 + v^2 = 1 \tag{3.93c}$$

Equation (3.93a) represents a plane $\mathcal{P}$ parallel to the d_1-axis in the (u, v, d_1)-space, while eq.(3.93b) represents a hyperbolic paraboloid $\mathcal{H}$ in the same space. Moreover, eq.(3.93c) represents a cylinder $\mathcal{C}$ of unit radius and axis parallel to the d_1-axis, all foregoing items being shown in Figs. 3.13a & b.

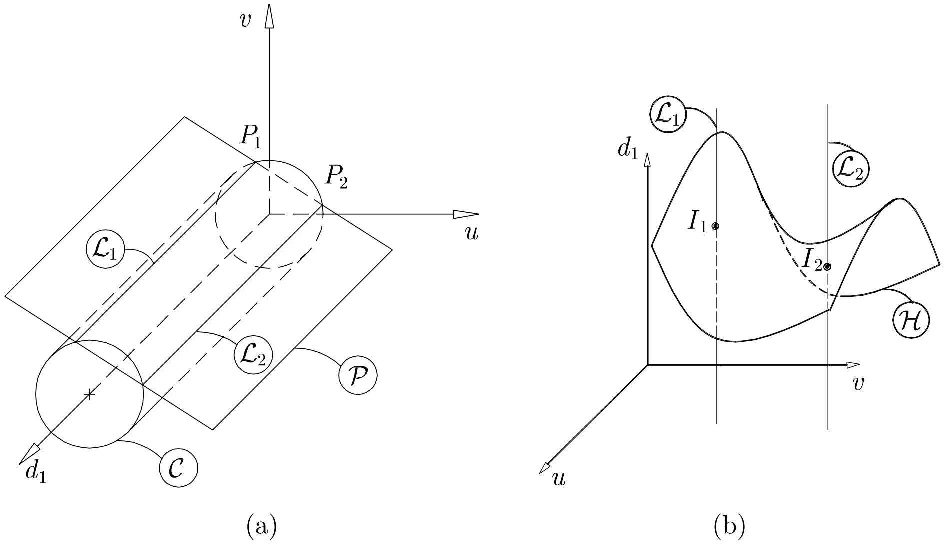

Figure 3.13: Intersections of (a) $\mathcal{P}$ and $\mathcal{C}$; and (b) $\mathcal{L}_i$ and $\mathcal{H}$, for $i = 1, 2$

The three-dimensional interpretation of eqs.(3.93a–c) is illustrated in Figs. 3.13(a) and (b), whereby line $\mathcal{L}_i$, for $i = 1, 2$, is defined by the intersection of the plane of eq.(3.93a) with the cylinder (3.93c). Moreover, each line $\mathcal{L}_i$ intersects the paraboloid (3.93b) at one single point, as illustrated in Fig. 3.13b, and as made apparent below.

The system of equations (3.93a–c) should be solved for u, v and d_1 in order to calculate the two conjugate output angles and their corresponding output translations. The intersections $\mathcal{L}_1$ and $\mathcal{L}_2$ of the plane $\mathcal{P}$ and the cylinder intersect the u-v plane at points P_1 and P_2, as shown in Fig. 3.13a, while $\mathcal{L}_1$ and $\mathcal{L}_2$ intersect the hyperbolic paraboloid $\mathcal{H}$ at points I_1 and I_2, as depicted in Fig. 3.13b. The intersection points P_1 and P_2 thus yield the two conjugate output angles ϕ_1 and ϕ_2. Once the two conjugate solutions u and v are known, via the coordinates of P_1 and P_2, the unique value of d_1 corresponding to each solution, and defining the intersection points I_1 and I_2, is determined from eq.(3.93b), namely,

$$d_1(\psi) = \frac{A_o u + C_o}{Av - Bu}, \quad Av \neq Bu \tag{3.94}$$

where we have dispensed with the argument ψ in coefficients A, A_o, B and C_o for simplicity.

Note that the denominator of eq.(3.94) vanishes if $Av = Bu$; then, as can be readily verified, the numerator of d_1 in the above expression vanishes as well, and d_1 is indeterminate. In this case, the surface $\mathcal{H}$ disappears for all values of the output translations d_1 and we are left with the plane $\mathcal{P}$ and the cylinder $\mathcal{C}$, which means that d_1 is free to take any value. That is, the motion of this linkage in the plane normal to its joint axes is independent of the translations along these axes. We are here in the presence of a parametric singularity producing a degeneracy of the linkage, similar to those described for the planar and spherical linkages in Subsections 3.4.1 and 3.4.2. Under this singularity, all joint axes are parallel ($\alpha_i = 0, i = 1, \ldots, 4$) and, hence, the coupler and the output links can freely slide along their cylindrical-joint axes.

Canonical Equation of the Hyperbolic Paraboloid $\mathcal{H}$

In order to gain insight into the problem geometry, we derive below the canonical equation of $\mathcal{H}$. To this end, we let

$$\mathbf{x} \equiv [\begin{array}{ccc} u & v & d_1 \end{array}]^T, \quad Q(\mathbf{x}) \equiv A_o u + B d_1 u - A d_1 v + C_o = 0$$

where $Q(\mathbf{x})$ is taken from eq.(3.93b), its Hessian matrix $\mathbf{H}$ then being

$$\mathbf{H} \equiv \frac{\partial^2 Q}{\partial \mathbf{x}^2} = \begin{bmatrix} 0 & 0 & B \\ 0 & 0 & -A \\ B & -A & 0 \end{bmatrix} \tag{3.95}$$

whose eigenvalues are readily computed as

$$\lambda_1 = -\sqrt{A^2 + B^2}, \quad \lambda_2 = 0\ , \quad \lambda_3 = \sqrt{A^2 + B^2}$$

The corresponding non-normalized eigenvectors $\mathbf{e}_i$, for $i = 1, 2, 3$, are

$$\mathbf{e}_1 = \begin{bmatrix} B \\ -A \\ \sqrt{A^2 + B^2} \end{bmatrix}, \quad \mathbf{e}_2 = \begin{bmatrix} A \\ B \\ 0 \end{bmatrix}, \quad \mathbf{e}_3 = \begin{bmatrix} -B \\ A \\ \sqrt{A^2 + B^2} \end{bmatrix}$$

and hence, the canonical equation of the surface $\mathcal{H}$ is of the form:

$$\zeta = \frac{\xi^2}{K} - \frac{\eta^2}{K}, \quad K = \frac{2A_o A}{A^2 + B^2}$$

where

$$\begin{aligned} \xi &= \frac{-\sqrt{2}}{2\sqrt{A^2 + B^2}} \left[Bu + Av + d_1 + \frac{A_o B}{4A_o A} \right] \\ \eta &= \frac{\sqrt{2}}{4\sqrt{A^2 + B^2}} \left(Bu - Av + d_1 + \frac{A_o B}{A_o A} \right) \\ \zeta &= \frac{1}{\sqrt{A^2 + B^2}} \left[Au + Bv + \frac{(A^2 + B^2) C_o A}{A_o A} \right] \end{aligned}$$

which proves that $\mathcal{H}$ is indeed a hyperbolic paraboloid.

The Case of d_1 Acting as Input

We include here a case that has been overlooked in the literature. In this case we regard the translational displacement of the output C joint of a RCCC linkage as input, the two outputs being angles ψ and ϕ. The problem no longer leads to a quadratic equation, but rather to a system of one quartic and one quadratic equations in two variables, as described presently.

Equations (3.93a & b) are both linear in u and v, which allows us to solve for these variables in terms of d_1, namely,

$$u = u(p,q) = \frac{-BC_o - CAd_1}{BA_o + B^2d_1 + A^2d_1} \tag{3.96a}$$

$$v = v(p,q) = \frac{-CA_o - AC_o + CBd_1}{BA_o + B^2d_1 + A^2d_1} \tag{3.96b}$$

where, in light of eqs.(3.91a), with $p = \cos\psi$ and $q = \sin\psi$, u and v become functions of p and q. The latter, moreover, are subject to

$$p^2 + q^2 = 1 \tag{3.97}$$

Substituting the values of u and v given above into eq.(3.93c) produces an equation free of u and v or, correspondingly, free of ϕ, namely,

$$f(p,q) = 0 \tag{3.98}$$

From eq.(3.72b) and eqs.(3.91a–c), both u and v, as given by eqs.(3.96a & b), are rational functions in these variables, with both numerator and denominator quadratic in p and q. Hence, u^2 and v^2 are rational functions with both numerator and denominator quartic in p and q. Therefore, $f(p,q) = 0$ leads, after clearing denominators, to a quartic equation in p and q.

The system of polynomial equations (3.97) and (3.98) apparently has a Bezout number of $4 \times 2 = 8$.

Numerical Examples

The foregoing algorithm is validated with two numerical examples. All numerical and symbolic calculations were completed with the aid of computer algebra.

Example 1: The Yang and Freudenstein Linkage

The first example is taken from (Yang and Freudenstein, 1964), with data as listed in Table 3.2. The output displacements, which vary with the input angle, are recorded in Table 3.3. For conciseness, we list only the results for $0 \leq \psi \leq \pi$. Our results match those reported by Yang and Freudenstein, considering the difference of input and output angles in both works, as explained in Subsections 3.2.4. It is noteworthy that only two displacement equations need be solved in our method, as compared with the system of six equations in six unknowns formulated by Yang and Freudenstein, within a purely numerical approach.

Example 2: Prescribing d_1 as Input

Table 3.2: D-H parameters of a RCCC mechanism

Link	1	2	3	4
a_i[in]	5	2	4	3
α_i[deg]	60	30	55	45
d_i[in]	0	variable	variable	variable

Table 3.3: RCCC displacements

	Branch 1		Branch 2	
ψ[deg]	ϕ[deg]	d_1[in]	ϕ[deg]	d_1[in]
0	83.70015289	−0.1731633183	−83.70015289	0.1731633183
20	68.59658457	0.01107737578	−105.3298310	0.8429100445
40	64.21379652	−0.5291731100	235.9479009	1.085719194
60	67.55907283	−1.262205018	223.0109192	0.9378806915
80	75.72376603	−1.888758476	214.5328380	0.6631677103
100	87.21970033	−2.259417488	209.1315343	0.3676536240
120	101.1949772	−2.248309766	206.1460158	0.08437533590
140	116.6745934	−1.770565950	205.6297490	−0.1502382358
160	131.8997404	−0.9205435228	208.4003706	−0.2203697101
180	144.2093802	−0.1150813726	215.7906198	0.1150813650

Table 3.4: Possible values of ψ and ϕ

	$[p, q]$	ψ[deg]	ϕ[deg]
1	$[0.6047587377, -.7964087325]$	-52.78	$[-65.68, -227.07]$
2	$[-.9289796338, -.3701308418]$	-158.27	$[-130.66, -207.99]$
3	$[0.5819053587, 0.8132565115]$	54.41	$[66.04, 226.10]$
4	$[0.8869350365, 0.4618941881]$	27.50	$[65.79, -113.02]$

In the second example, we try to find the rotations, ψ and ϕ, for a given d_1, and given dimensions of a RCCC linkage. The dimensions are the same as those in Example 1, with $d_1 = 1.0$. In this example, eq.(3.98) takes the form:

$$A_0 p^4 + A_1(q)p^3 + A_2(q)p^2 + A_3(q)p + A_4(q) = 0 \tag{3.99}$$

where coefficients $A_i(q)$, for $i = 0, \ldots, 4$, are given below:

$$\begin{aligned}
A_0 &= 0.09209746694 \\
A_1(q) &= -0.06765823468q - 0.0073324502 \\
A_2(q) &= -0.1754806581q^2 + 0.01487658368q - 0.1902460942 \\
A_3(q) &= 0.1353164694q^3 + 0.1202907568q^2 + 0.2424947249q + 0.04203177757 \\
A_4(q) &= -0.015625q^4 - 0.0811898817q^3 - 0.020697377q^2 - 0.1362382267q \\
&\quad + 0.0484753242
\end{aligned}$$

Equation (3.99) represents a curve in the p-q plane, whose intersections with the circle of eq.(3.97) yield all real roots of the system at hand. Note, moreover, that all such roots are bound to lie on the above circle. The four real solutions of the foregoing system are given by the four intersections depicted in Fig. 3.14. The solutions are listed in Table 3.4, including the corresponding angles of rotation[4].

Mobility of the Input and Output Links

In this case, the mobility analysis applies *only to the input ψ and the output ϕ*, as this analysis decides whether a joint is fully rotatable—can sweep an angle of 2π—or not. This analysis thus reduces to that of the spherical mechanism whose IO equation is the primal part of the dual equation of this linkage.

[4] In this table only p and q are given with 10 digits; all other values are given with only four, for the sake of economy of space.

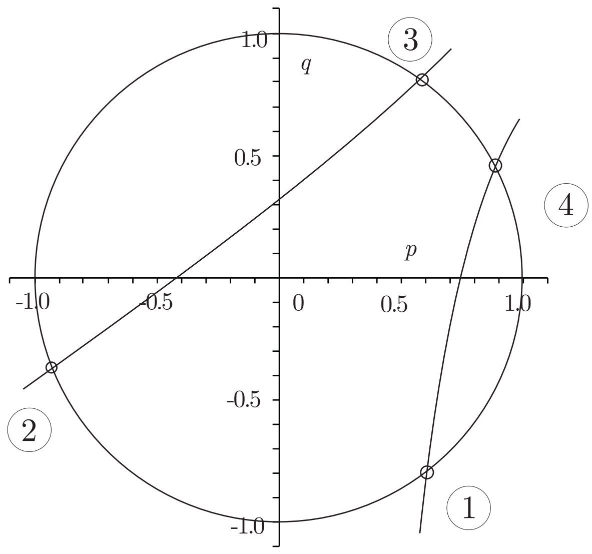

Figure 3.14: The case of an input translation

3.5 Approximate Synthesis

Regardless of the type of linkage, $\mathbf{k}$ is a n-dimensional vector of Freudenstein parameters. For planar linkages $n = 3$; for spherical linkages, $n = 4$, while for spatial linkages of the RCCC type[5], $n = 8$. In general, for $m > n$, no set of values $\{k_i\}_1^n$ can verify all m synthesis equations. We thus have an *error vector* $\mathbf{e}$:

$$\mathbf{e} \equiv \mathbf{b} - \mathbf{S}\mathbf{k} \tag{3.100a}$$

which, in the case of RCCC linkages, becomes dual, i.e.,

$$\hat{\mathbf{e}} \equiv \hat{\mathbf{b}} - \hat{\mathbf{S}}\hat{\mathbf{k}} \tag{3.100b}$$

The foregoing error vector, in its two versions, real and dual, is termed the *design-error vector*. A positive scalar derived from this vector will be termed a *design error*.

The *design error* e_d adopted here is the rms value of the components of vector $\mathbf{e}$, i.e.,

$$e_d \equiv \sqrt{\frac{1}{m}\sum_1^m e_i^2} \tag{3.101a}$$

where e_i is the ith component of vector $\mathbf{e}$, i.e., the *residual* of the ith synthesis equation. Hence, the design error is proportional to the Euclidean norm of the design-error vector:

$$e_d \equiv \sqrt{\frac{1}{m}}\,\|\mathbf{e}\| \tag{3.101b}$$

[5]For this type of linkage, two input-output relations are available: the input is the same in both, but the prescribed output comprises both the rotation and the translation of the C joint.

It is apparent that, for fixed m, if we minimize $\|\mathbf{e}\|$, we minimize e_d. In the case of the spatial four-bar linkage, of course, e_d is defined as

$$\hat{e}_d = \sqrt{\frac{1}{m}}\,\|\hat{\mathbf{e}}\| \tag{3.101c}$$

where, from eq.(A.9e),

$$\|\hat{\mathbf{e}}\| = \sqrt{\hat{\mathbf{e}}^T\hat{\mathbf{e}}}, \quad \hat{\mathbf{e}}^T\hat{\mathbf{e}} = \|\mathbf{e}\|^2 + \epsilon 2\mathbf{e}^T\mathbf{e}_o \tag{3.101d}$$

The value $\mathbf{k}_0$ of $\mathbf{k}$ that minimizes $\|\mathbf{e}\|$, as derived in Subsection 1.4, is applicable to the planar and spherical cases; it is given in eq.(1.41)[6]—The value $\hat{\mathbf{k}}_0$ that minimizes $\hat{e}_d$ is discussed in Subsection 3.5.3. In the planar and spherical cases, this equation leads to

$$\mathbf{k}_0 = \mathbf{S}^I\mathbf{b} \tag{3.102a}$$

which is the *least-square approximation* of the given overdetermined system of linear equations, $\mathbf{S}^I$ being the left Moore-Penrose generalized inverse of $\mathbf{S}$, as introduced in eq.(1.42), and is given by

$$\mathbf{S}^I = (\mathbf{S}\mathbf{S}^T)^{-1}\mathbf{S}^T \tag{3.102b}$$

Hence,

$$\mathbf{e}_0 \equiv \mathbf{b} - \mathbf{S}\mathbf{k}_0 \tag{3.103}$$

is the *least-square error vector*, and

$$e_{d0} \equiv \sqrt{\frac{1}{m}}\,\|\mathbf{e}_0\| \tag{3.104}$$

is the *least-square design error* of the approximation to the overdetermined system of synthesis equations.

Remark 3.5.1 *Expression (3.102a) for* $\mathbf{k}_0$ *can be derived upon multiplying both sides of eq.(3.12) by* $\mathbf{S}^T$*:*

$$(\mathbf{S}^T\mathbf{S})\mathbf{k} = \mathbf{S}^T\mathbf{b} \tag{3.105}$$

where $\mathbf{S}^T\mathbf{S}$ *is a* $n \times n$ *matrix. If this matrix is nonsingular, then*

$$\mathbf{k} \equiv \mathbf{k}_0 = (\mathbf{S}^T\mathbf{S})^{-1}\mathbf{S}^T\mathbf{b}$$

Remark 3.5.2 *The least-square approximation* $\mathbf{k}_0$ *can be thought of as being derived upon "inverting" the rectangular* $\mathbf{S}$ *matrix in the original overdetermined system, eq.(3.12), with the "inverse" of* $\mathbf{S}$ *understood in the generalized sense.*

Remark 3.5.3 $\mathbf{k}_0$ *minimizes the Euclidean norm of* $\mathbf{e}$*, which is proportional to the* design error.

[6] $\mathbf{k}_0$ shouldn't be mistaken by $\mathbf{k}_o$, the dual part of $\hat{\mathbf{k}}$.

Remark 3.5.4 *The least-square error of the approximation of the overdetermined system of synthesis equations* does not *measure the* positioning error*, a.k.a. the* structural error*, but rather the design error* $\mathbf{e}$ *defined above. The structural error produced by the synthesized linkage must be measured with respect to the task, not with respect to the synthesis equations. That is, if we let* $\overline{\phi}_i$ *denote the* prescribed *value of the output angle, corresponding to the* ψ_i *value, with* ϕ_i *denoting the* generated *value of the output angle, then the structural error is the vector* $\mathbf{s}$ *given by*

$$\mathbf{s} \equiv [\,\phi_1 - \overline{\phi}_1 \quad \phi_2 - \overline{\phi}_2 \quad \cdots \quad \phi_m - \overline{\phi}_m\,]^T \tag{3.106}$$

Computing the least-square approximation $\mathbf{k}_0$ *verbatim* as appearing in eq.(3.102a) *is not advisable* because of Remark 1.4.3 and the discussion in the paragraph below this remark. This is, if $\kappa(\mathbf{S})$ is moderately large, say, of the order of 1000, $\kappa(\mathbf{S}^T\mathbf{S})$ is inadmissibly large, of the order of 10^6.

Alternatives to the solution of eq.(3.12) in the presence of a rectangular $\mathbf{S}$ exist (Golub and Van Loan, 1983), as outlined in Subsection 1.4.5 and implemented in scientific software. The two methods outlined in Subsection 1.4.5 fall into what is called the *QR decomposition*: $\mathbf{S}$ is factored into an orthogonal matrix $\mathbf{Q}$ and an upper-triangular matrix $\mathbf{R}$.

Maple uses Householder reflections to find numerically the least-square approximation of an overdetermined system of linear equations; it uses Gram-Schmidt orthogonalization to do the same if data are given *symbolically*.

In any event, the original system (3.12) is transformed into the form

$$\mathbf{T}\mathbf{k} = \mathbf{c} \tag{3.107}$$

where $\mathbf{T}$ and $\mathbf{c}$ are the transforms of $\mathbf{S}$ and $\mathbf{b}$ of eq.(3.100a), respectively, with $\mathbf{T}$ of the form

$$\mathbf{T} = \begin{bmatrix} \mathbf{U} \\ \mathbf{O} \end{bmatrix} \tag{3.108}$$

while $\mathbf{U}$ and $\mathbf{O}$ are

$$\mathbf{U} = \begin{bmatrix} u_{11} & u_{12} & \cdots & u_{1n} \\ 0 & u_{22} & \cdots & u_{2n} \\ \vdots & \vdots & \ddots & \vdots \\ 0 & 0 & \cdots & u_{nn} \end{bmatrix}, \quad \mathbf{O}: \quad (m-n) \times n \;\; \text{zero matrix} \tag{3.109}$$

In order to solve eq.(3.107) for $\mathbf{k}$, we partition vector $\mathbf{c}$ into a n-dimensional upper part $\mathbf{c}_U$ and a $(m-n)$-dimensional lower part $\mathbf{c}_L$:

$$\mathbf{c} = \begin{bmatrix} \mathbf{c}_U \\ \mathbf{c}_L \end{bmatrix} \tag{3.110}$$

where, in general, $\mathbf{c}_L \neq \mathbf{0}$.

System (3.107) thus takes the form

$$\begin{bmatrix} \mathbf{U} \\ \mathbf{O} \end{bmatrix} \mathbf{k} = \begin{bmatrix} \mathbf{c}_U \\ \mathbf{c}_L \end{bmatrix} \quad \Rightarrow \quad \begin{cases} \mathbf{U}\mathbf{k} = \mathbf{c}_U \\ \mathbf{O}\mathbf{k} = \mathbf{c}_L \neq \mathbf{0} \end{cases} \tag{3.111}$$

Remark 3.5.5 *If* $\mathbf{S}$ *is of full rank, then so is* $\mathbf{T}$ *and hence,* $\mathbf{U}$ *is nonsingular.*

Remark 3.5.6 *If* $\mathbf{U}$ *is nonsingular, then none of its diagonal entries vanishes, for* $\det(\mathbf{U}) = u_{11}u_{22}\cdots u_{nn}$.

Remark 3.5.7 *If* $\mathbf{U}$ *is nonsingular, then* $k_1,\ k_2,\ \ldots,\ k_n$ *can be computed from the first of eqs.(3.111) by* backward substitution.

Remark 3.5.8 *The second of eqs.(3.111) is a contradiction: its RHS is zero, but its LHS is not! Hence,* $\mathbf{c}_L$ *is the error vector—although not in the original vector basis, but in a new, orthonormal basis—and thus, the error in the approximation of the synthesis equations is*

$$e_{d0} = \sqrt{\frac{1}{m}}\|\mathbf{c}_L\| \tag{3.112}$$

3.5.1 The Approximate Synthesis of Planar Four-Bar Linkages

For planar linkages the procedure is straightforward, as illustrated with the example below.

Example 3.5.1 (Approximate synthesis of the gripper mechanism) *Synthesize the actuation mechanism of Fig. 3.6, but now with a large number of input-output (IO) values. For comparison purposes, the data points used by Dudiţă et al. (1989) are used here, which are prescribed by equally spacing 61 IO values between* $\psi_1 = 30°$, $\phi = 240°$ *and* $\psi_{61} = 60°$, $\phi_{61} = 210°$, *as depicted in Fig. 3.15.*
Solution*: The* 61×3 *synthesis matrix* $\mathbf{S}$ *and the 61-dimensional vector* $\mathbf{b}$ *are not displayed because of economy of space. Details of the solution are available in the code written for the purpose at hand*[7]*. The least-square approximation was computed using Householder reflections, which yielded, with 16 digits for comparison purposes with the results reported by Dudiţă et al. (1989):*

$$\mathbf{k}_0 = [\,2.9417068638 \quad 2.7871366821 \quad 2.7869959265\,]^T$$

with corresponding link lengths

$$a_1 = 1.0, \quad a_2 = 0.3587911588, \quad a_3 = 0.7071482506, \quad a_4 = 0.3588092794$$

[7] See `DuditaApproxSynth.ms`

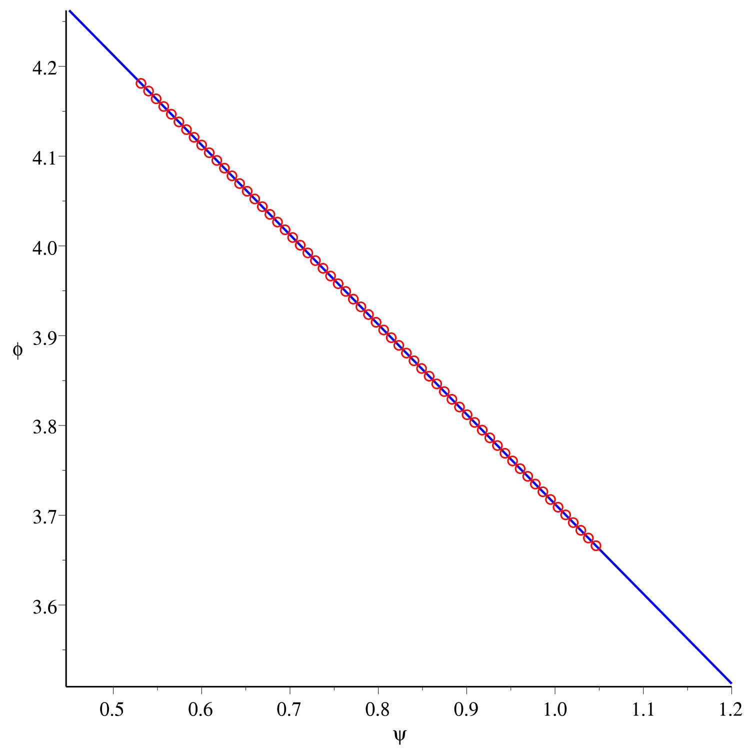

Figure 3.15: The 61 points prescribed in the ϕ-vs.-ψ plane

in units of length. In the foregoing reference, the authors computed the least-square approximation using the normal equations*, which produced*

$$\mathbf{k}_D = [\,2.9398767070 \quad 2.7857633820 \quad 2.7857633820\,]^T$$

which led to the link lengths[8]

$$a_1 = 1.0, \quad a_2 = 0.3589680324, \quad a_3 = 0.7071510069, \quad a_4 = a_2$$

in units of length. The values of both $\mathbf{k}$ *and* $\mathbf{k}_D$ *coincide up to the first two digits, those of the link lengths up to the first three digits, which is a fair matching, a consequence of the moderate condition number of the synthesis matrix, namely* $\kappa = 195$*, as computed in* `Dudita2.mw`*. However, the normality conditions were met, with the values provided in the foregoing reference, with an error of* $O(-4)$*; the same conditions were met with an error of* $O(-14)$ *in the code given above, which uses HHR.*

To the naked eye, the synthesized linkage doesn't appear different from that in Fig. 3.7.

[8]Dudiţă et al. adjusted the values of the second and the third components of the $\mathbf{k}_D$ array to be identical.

3.5.2 The Approximate Synthesis of Spherical Linkages

This case parallels that of planar linkages, with the provision that, as in the case of exact synthesis of spherical linkages, nothing guarantees that the computed least-square approximation complies with the two conditions (3.33). The first of these, $|k_3| \leq 1$, can be enforced in the least-square solution by adding one more equation, $k_3 = 0$, to the synthesis equations. Compliance with this condition, however, will invariably lead to a larger value of e_{d0}. Enforcing the second condition of eq.(3.33) is less straightforward, as it requires techniques for solving problems of *constrained least squares* with nonlinear equality constraints, which fall outside of the scope of this course, and will not be further discussed. The reader is referrred to the literature on engineering optimization whenever confronted with this problem.

Adjoining the above equation, $k_3 = 0$, to the synthesis equation, then, leads to the *augmented synthesis equations*

$$\mathbf{S}_a \mathbf{k} = \mathbf{b}_a \tag{3.113a}$$

where

$$\mathbf{S}_a = \begin{bmatrix} \mathbf{S} \\ \mathbf{u}^T \end{bmatrix}, \quad \mathbf{b}_a = \begin{bmatrix} \mathbf{b} \\ 0 \end{bmatrix} \tag{3.113b}$$

with $\mathbf{u} = [0,\, 0,\, 1,\, 0]^T$, and hence, $\mathbf{S}_a$ now becomes of $(m+1) \times 4$, while $\mathbf{b}_a$ is now $(m+1)$-dimensional.

But least-square approximations allow for more flexibility, if we introduce *weights* in eq.(3.113a), by means of a $(m+1) \times (m+1)$ constant matrix $\mathbf{V}_a$:

$$\mathbf{V}_a \mathbf{S}_a \mathbf{k} = \mathbf{V}_a \mathbf{b}_a \tag{3.114a}$$

with

$$\mathbf{V}_a = \begin{bmatrix} \mathbf{V} & \mathbf{0}_m \\ \mathbf{0}_m{}^T & v \end{bmatrix} \tag{3.114b}$$

in which $\mathbf{V}$ is a $m \times m$ block, $\mathbf{0}_m$ is the m-dimensional zero matrix, and v is a scalar. Both $\mathbf{V}$ and v are assigned by the user under the only constraint of avoiding the introduction of large roundoff-error amplification. We will describe presently how to prescribe $\mathbf{V}$ and v.

Notice that the least-square approximation $\mathbf{k}_0$ of eq.(3.114a) now becomes, symbolically,

$$\begin{aligned} \mathbf{k}_0 &= [(\mathbf{V}_a \mathbf{S}_a)^T (\mathbf{V}_a \mathbf{S}_a)]^{-1} (\mathbf{V}_a \mathbf{S}_a{}^T) \mathbf{V}_a \mathbf{b}_a \\ &= (\mathbf{S}_a{}^T \mathbf{W}_a \mathbf{S}_a)^{-1} \mathbf{S}_a{}^T \mathbf{W}_a \mathbf{b}_a, \quad \mathbf{W}_a \equiv \mathbf{V}_a{}^T \mathbf{V}_a \end{aligned} \tag{3.115}$$

in which the symmetric and positive-definite $\mathbf{W}_a$ is termed a *weighting matrix*.

Also notice that

$$\mathbf{W}_a = \begin{bmatrix} \mathbf{V}^T & \mathbf{0}_m \\ \mathbf{0}_m{}^T & v_{m+1} \end{bmatrix} \begin{bmatrix} \mathbf{V} & \mathbf{0}_m \\ \mathbf{0}_m{}^T & v_{m+1} \end{bmatrix} = \begin{bmatrix} \mathbf{W} & \mathbf{0}_m \\ \mathbf{0}_m{}^T & w_{m+1} \end{bmatrix} \tag{3.116a}$$

with

$$\mathbf{W} = \mathbf{V}^T\mathbf{V}, \quad w_{m+1} \equiv v_{m+1}^2 \tag{3.116b}$$

Since no constraint is imposed on $\mathbf{V}$, besides robustness to round-off error amplification, $\mathbf{V}$ can be freely chosen as *symmetric and positive-definite*, and hence, nonsingular, i.e.,

$$\mathbf{V}^2 = \mathbf{W} \quad \Rightarrow \mathbf{V} = \sqrt{\mathbf{W}} \tag{3.117a}$$

where $\sqrt{\mathbf{W}}$ denotes the *the positive-definite square root of* $\mathbf{W}$. Now, the simplest matrices to square-root are diagonal matrices, $\mathbf{W}$ then being chosen as

$$\mathbf{W} = \mathrm{diag}(w_1,\, w_2,\, \ldots,\, w_m) \tag{3.117b}$$

Now, the error vector in the approximation of eqs.(3.114a) is

$$\mathbf{e}_a = \mathbf{V}_a(\mathbf{b}_a - \mathbf{S}_a\mathbf{k}) = \begin{bmatrix} \mathbf{V} & \mathbf{0}_m \\ \mathbf{0}_m{}^T & v_{m+1} \end{bmatrix} \begin{bmatrix} \mathbf{b} - \mathbf{S}\mathbf{k} \\ k_3 \end{bmatrix} \tag{3.118a}$$

whose Euclidean norm is

$$\begin{aligned} \|\mathbf{e}_a\|^2 &= [\, \mathbf{b}^T - \mathbf{k}^T\mathbf{S}^T \quad k_3 \,] \begin{bmatrix} \mathbf{V}^2 & \mathbf{0}_m \\ \mathbf{0}_m{}^T & v_{m+1}^2 \end{bmatrix} \begin{bmatrix} \mathbf{b} - \mathbf{S}\mathbf{k} \\ k_3 \end{bmatrix} \\ &= (\mathbf{b}^T - \mathbf{k}^T\mathbf{S}^T)\mathbf{W}(\mathbf{b} - \mathbf{S}\mathbf{k}) + w_{m+1}k_3^2 \\ &= \sum_{i=1}^{m} w_i e_i^2 + w_{m+1}k_3^2 \end{aligned} \tag{3.118b}$$

which thus yields a *weighted error-norm.* In order to avoid large roundoff-error amplification, we choose the weighting factors $\{\, w_i \,\}_1^{m+1}$ as

$$\sum_{i=1}^{m+1} w_i = 1, \quad 0 \le w_i \le 1, \quad i = 1, \ldots, m \tag{3.119}$$

so that $\|\mathbf{e}_a\|^2$ becomes a *convex combination* of all $m+1$ errors. If no preference is given to the set $\{\, e_i \,\}_1^m$, then the first m weights can be chosen all equal, while w_{m+1} is to be chosen so as to enforce $|k_3|$ to be smaller than unity but, if w_{m+1} is chosen unnecessarily large, then $|k_3|$ will be "too small" at the expense of a "large" design error. The best compromise is to be chosen by trial and error.

3.5.3 The Approximate Synthesis of Spatial Linkages

This subsubsection is largely based on (Angeles, 2012). The synthesis equations (3.50) for the spatial four-bar linkage are reproduced below for quick reference:

$$\mathbf{S}\mathbf{k} = \mathbf{b} \tag{3.120a}$$

$$\mathbf{S}\mathbf{k}_o = \mathbf{b}_o - \mathbf{S}_o\mathbf{k} \tag{3.120b}$$

which can be cast in the standard form (1.28) of an overdetermined system of linear equations, in this case of $2m$ equations in $2 \times 4 = 8$ unknowns, the four components of $\mathbf{k}$ and $\mathbf{k}_o$. Indeed, assembling the above equations into one single system yields

$$\underbrace{\begin{bmatrix} \mathbf{S} & \mathbf{O} \\ -\mathbf{S}_o & \mathbf{S} \end{bmatrix}}_{\mathbf{A}} \underbrace{\begin{bmatrix} \mathbf{k} \\ \mathbf{k}_o \end{bmatrix}}_{\mathbf{x}} = \underbrace{\begin{bmatrix} \mathbf{b} \\ \mathbf{b}_o \end{bmatrix}}_{\mathbf{r}} \tag{3.121}$$

whose matrix $\mathbf{A}$ has four $m \times 4$ blocks, while $\mathbf{x}$ is an eight-dimensional vector. One could think of submitting eq.(3.121) to a linear least-square solver and, sure enough, obtain a least-square solution $\mathbf{x}_0$ à la eq.(1.41). Problem is, this solution would be *meaningless* because the error $\mathbf{e} \equiv \mathbf{r} - \mathbf{Ax}$ **does not admit a norm**. The reason is that the first m components of $\mathbf{e}$ are dimensionless, as they refer to the spherical linkage associated with the spatial linkage at hand, while the last m bear units of length, as they refer to sliding errors. This approach is thus ruled out. Instead, the synthesis equations in dual form, eq.(3.45), with the definitions appearing in eq.(3.46), are recalled, as reproduced below for quick reference:

$$\hat{\mathbf{S}}\hat{\mathbf{k}} = \hat{\mathbf{b}} \tag{3.122}$$

which, for $m > 4$, cannot be satisfied exactly; the *dual error* incurred is

$$\hat{\mathbf{e}} = \hat{\mathbf{b}} - \hat{\mathbf{S}}\hat{\mathbf{k}} \tag{3.123}$$

Equation (3.122) can be shown to admit the least-square solution

$$\hat{\mathbf{k}}_0 = \hat{\mathbf{S}}^I\hat{\mathbf{b}}, \quad \hat{\mathbf{S}}^I = (\hat{\mathbf{S}}^T\hat{\mathbf{S}})^{-1}\hat{\mathbf{S}}^T \tag{3.124}$$

where

$$\hat{\mathbf{S}}^T\hat{\mathbf{S}} = \mathbf{S}^T\mathbf{S} + \epsilon(\mathbf{S}^T\mathbf{S}_o + \mathbf{S}_o^T\mathbf{S}) \tag{3.125}$$

whose inverse is readily computed using eq. (A.13) of the Appendix:

$$(\hat{\mathbf{S}}^T\hat{\mathbf{S}})^{-1} = (\mathbf{S}^T\mathbf{S})^{-1} - \epsilon(\mathbf{S}^T\mathbf{S})^{-1}(\mathbf{S}^T\mathbf{S}_o + \mathbf{S}_o^T\mathbf{S})(\mathbf{S}^T\mathbf{S})^{-1} \tag{3.126}$$

and hence,

$$\hat{\mathbf{S}}^I = \mathbf{S}^I + \epsilon[-\mathbf{S}^I\mathbf{S}_o\mathbf{S}^I + \underbrace{(\mathbf{S}^T\mathbf{S})^{-1}\mathbf{S}_o^T - (\mathbf{S}^T\mathbf{S})^{-1}\mathbf{S}_o^T\mathbf{S}\mathbf{S}^I}_{\boldsymbol{\Delta}}] \tag{3.127}$$

Were it not for the $\boldsymbol{\Delta}$ term in the above expression, it would mimic faithfully the expression for the dual inverse appearing in eq. (A.13). It will become apparent that this term can be dropped from the above expression, thereby a) simplifying the expression of interest and b) leading to a *minimum-size linkage*.

Upon substitution of expression (3.127) into eq.(3.124), and expansion of the expression thus resulting, the least-square solution $\hat{\mathbf{k}}_0$ is obtained as

$$\hat{\mathbf{k}}_0 = \underbrace{(\mathbf{S}^T\mathbf{S})^{-1}\mathbf{S}^T\mathbf{b}}_{\mathbf{k}_0} + \epsilon \underbrace{(\mathbf{S}^T\mathbf{S})^{-1}[\mathbf{S}_o^T\mathbf{b} + \mathbf{S}^T\mathbf{b}_o - (\mathbf{S}^T\mathbf{S}_o + \mathbf{S}_o^T\mathbf{S})(\mathbf{S}^T\mathbf{S})^{-1}\mathbf{S}^T\mathbf{b}]}_{\mathbf{k}_{o0}} \tag{3.128}$$

While the above expressions for the least-square solution of both the primal part of $\hat{\mathbf{k}}$, $\mathbf{k}_0$, and its dual counterpart $\mathbf{k}_{o0}$ are theoretically sound, they are not appropriate for computations verbatim, given the large amount of floating-point operations involved, and their need of the inverse of $\mathbf{S}^T\mathbf{S}$. As pointed out in Remark 1.4.3, it is not advisable to compute verbatim that inverse because of the likely amplification of the condition number of the matrix product. It will be made apparent in the sequel that a terser solution $\mathbf{k}_{o0}$ can be obtained.

Indeed, if first the least-square solution $\mathbf{k}_0$ for the primal part of $\hat{\mathbf{k}}$ is computed from eq.(3.120a), using the left Moore-Penrose generalized inverse $\mathbf{S}^I$, and then this expression is substituted into eq.(3.120b), the least-square solution $\mathbf{k}_{o0}$ is derived as

$$\mathbf{k}_{o0} = \mathbf{S}^I(\mathbf{b}_o - \mathbf{S}_o\mathbf{S}^I\mathbf{b}) \tag{3.129}$$

which is much terser than its counterpart expression in eq.(3.128). The difference between the two expressions can be explained based on the observation that the dual generalized inverse $\hat{\mathbf{S}}^I$ *is not unique*, contrary to its real counterpart. This fact is made apparent below.

Paraphrasing the derivation of the expression (A.13) for the dual inverse, let $\hat{\mathbf{B}} = \mathbf{B} + \epsilon\mathbf{B}_o$ be the generalized inverse of a $m \times n$ dual matrix $\hat{\mathbf{A}} = \mathbf{A} + \epsilon\mathbf{A}_o$, with $m > n$. As $\hat{\mathbf{A}}$ has been assumed of $m \times n$, $\hat{\mathbf{B}}$ is bound to be of $n \times m$.

Then,

$$\hat{\mathbf{B}}\hat{\mathbf{A}} = \mathbf{1}_n \tag{3.130}$$

with $\mathbf{1}_n$ denoting the $n \times n$ identity matrix. Upon expansion of the left-hand side of the above equation, two real equations are obtained, one for the primal, one for the dual part:

$$\mathbf{B}\mathbf{A} = \mathbf{1}_n, \quad \mathbf{B}_o\mathbf{A} + \mathbf{B}\mathbf{A}_o = \mathbf{O}_n \tag{3.131}$$

the first equation leading to the not so unexpected result $\mathbf{B} = \mathbf{A}^I$, which, when substituted into the second equation, yields a matrix equation for $\mathbf{B}_o$:

$$\mathbf{B}_o\mathbf{A} = -\mathbf{A}^I\mathbf{A}_o$$

A more suitable form of the above equation is obtained, with the unknown $\mathbf{B}_o$ as the right-hand factor of the left-hand side upon transposing the two sides of the equation, namely,

$$\mathbf{A}^T\mathbf{B}_o^T = -\mathbf{A}_o^T(\mathbf{A}^I)^T \equiv -\mathbf{A}_o^T\mathbf{A}(\mathbf{A}^T\mathbf{A})^{-1}$$

which is a system of n^2 equations in $m \times n > n^2$ unknowns. The system is, thus, underdetermined, thereby admitting infinitely many solutions. The conclusion is, then, that the dual left generalized inverse is not unique. Among all that many solutions, one of minimum *Frobenius* norm can be obtained if one resorts to the right Moore-Penrose generalized inverse of $\mathbf{A}^T$, denoted $(\mathbf{A}^T)^\dagger$ (Nash and Sofer, 1996):

$$(\mathbf{A}^T)^\dagger = \mathbf{A}(\mathbf{A}\mathbf{A}^T)^{-1} \tag{3.132}$$

After some obvious manipulations,

$$\mathbf{B}_o = -\mathbf{A}^I\mathbf{A}_o\mathbf{A}^I \tag{3.133}$$

Therefore, the minimum-Frobenius-norm $\hat{\mathbf{A}}^I$ is

$$\hat{\mathbf{A}}^I = \mathbf{A}^I - \epsilon\mathbf{A}^I\mathbf{A}_o\mathbf{A}^I \tag{3.134}$$

The reader is invited to show that, if the foregoing formula is applied to compute the least-square solution $\hat{\mathbf{k}}_0$, the expression below is obtained:

$$\hat{\mathbf{k}}_0 = \mathbf{S}^I\mathbf{b} + \epsilon\mathbf{S}^I(\mathbf{b}_o - \mathbf{S}_o\mathbf{S}^I\mathbf{b}) \tag{3.135}$$

whose dual part is exactly the one obtained in eq.(3.129). By the same token, the reader is invited to prove that $\mathbf{\Delta}^T$, with $\mathbf{\Delta}$ as appearing in eq.(3.127), is *an orthogonal complement* (OC) of $\mathbf{S}^T$, which is the reason why this term was filtered out in eq.(3.129). Below we expand on the OC concept.

Given a $m \times n$ matrix $\mathbf{M}$, with $m < n$, i.e., with more columns than rows—for simplicity, its m rows will be assumed linearly independent—its ith row can be regarded as a vector $\mathbf{m}_i \in \mathbb{R}^n$. Since $\mathbf{M}$ has m such vectors, it is possible to find $n-m$ linearly independent vectors $\{\,\mathbf{p}_k\,\}_1^{n-m}$ orthogonal to the m rows—picture this with $m = 2$ and $n = 3$. If the vectors of this set are arrayed as the columns of a $n \times (n-m)$ matrix $\mathbf{P}$, then

$$\mathbf{MP} = \mathbf{O}_{mn'} \tag{3.136}$$

where $\mathbf{O}_{mn'}$ denotes the $m \times (n-m)$ zero matrix. Every matrix $\mathbf{P}$ that verifies eq.(3.136) is termed an orthogonal complement of $\mathbf{M}$. It follows that *the OC is not unique*. Indeed, an rearrangement of the columns of $\mathbf{P}$ yields another OC of $\mathbf{M}$. Likewise, any multiple of a given $\mathbf{P}$ is also an OC of $\mathbf{M}$.

In summary, then, the approximate synthesis of a RCCC linkage proceeds sequentially:

1. Decouple the synthesis problem into two subproblems: one leading to the optimum Freudenstein parameters of the spherical linkage associated with the spatial linkage of interest, eq.(3.120a), the other with the optimum dual counterparts of the foregoing parameters, eq.(3.120b).

2. Apply Householder reflections to the primal part $\mathbf{S}$ of the dual synthesis matrix, thereby obtaining a $m \times m$ orthogonal matrix $\mathbf{H}$ and a $m \times 4$ matrix $\mathbf{E}$, with an upper-triangular 4×4 block occupying its first four rows and a $(m-4) \times 4$ block of zeros. Apply the same reflections to $\mathbf{b}$ of the right-hand side of eq.(3.120a) and obtain $\mathbf{k}_0$ by forward substitution on the first four equations.

3. Substitute $\mathbf{k}$ into eq.(3.120b) with $\mathbf{k}_0$ and then apply the same Householder reflections to the right-hand side of the same equations.

4. Compute $\mathbf{k}_{o0}$ from the transformed eqs.(3.120b) by backward substitution over the same 4×4 block.

5. Compute the skew angles $\{ \alpha_i \}_1^4$ from eqs.(3.32a)–(3.32d) by nonlinear-equation solving.

6. Compute the distances $\{ a_i \}_1^4$ from eqs.(3.42) by linear-equation solving.

7. Done!

3.6 Linkage Performance Evaluation

3.6.1 Planar Linkages: Transmission Angle and Transmission Quality

A variable of merit that is used to assess the linkage performance is the *transmission angle* μ, illustrated in Fig. 3.1. The transmission angle is thus defined as *the angle between the axes of the output and the coupler links.*

The relevance of this angle is apparent from a kinetostatic analysis[9]: in Fig. 3.16, the *internal forces of constraint* are indicated as F_{ij}, to denote the force exerted by the ith link on the jth link, using a standard terminology. Therefore, the force transmitted by the output link to the frame has a magnitude $|F_{41}|$ given by

$$|F_{41}| = |F_{14}| = |F_{34}| \tag{3.137}$$

where, from the static equilibrium of the coupler and the input links,

$$|F_{34}| = |F_{32}| = \left| \frac{\tau_\psi}{a_2 \sin(\psi - \theta)} \right| \tag{3.138}$$

and τ_ψ is the *applied torque* that *balances statically* the *load torque* τ_ϕ.

The magnitude of the radial component of F_{14}, denoted $|F_{14}|_r$, is derived upon substitution of eq.(3.138) into eq.(3.137), thus obtaining

$$|F_{14}|_r \equiv |F_{14} \cos \mu| = \left| \frac{\tau_\psi}{a_2 \sin(\psi - \theta)} \cos \mu \right| \tag{3.139}$$

from which it is apparent that $|F_{14}|_r$ is proportional to the magnitude of the applied moment and to the cosine of the transmission angle. Since this is a nonworking force, one is interested in keeping it as low as possible. However, it cannot be made zero by simply making zero the applied torque because, then, no useful force would be transmitted! Thus,

[9] This is an analysis of forces and moments of *a mechanical system in motion under static, conservative conditions.*

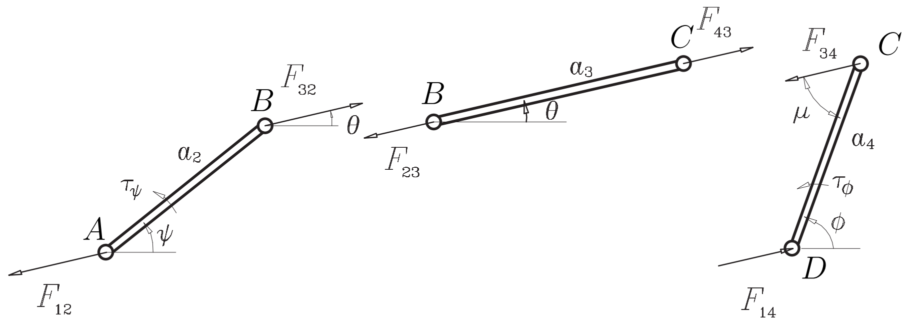

Figure 3.16: A static analysis of the four-bar linkage

the only possible way of keeping that force as small as possible is by keeping $\cos\mu$ as small as possible, i.e., by keeping μ as close as possible to $\pm 90°$.

The transmission angle is posture-dependent, of course; hence, it cannot be maintained at a fixed value for all the linkage postures. In practice, a minimum allowable value on the transmission angle or, rather, on its absolute value, is prescribed. This is commonly accepted as 45°, i.e., a specification when designing four-bar linkages is

$$|\mu| \geq 45° \tag{3.140}$$

If one is interested in a global evaluation of the performance of a four-bar linkage throughout its full range of motion, namely, $\psi_1 \leq \psi \leq \psi_2$, then a merit function of the linkage that takes into account *all possible postures* is needed. This quantity can be fairly termed the *transmission quality* of the linkage, which is defined as the *root-mean-square* (rms) value of $\sin\mu$:

$$Q \equiv \sqrt{\frac{1}{\Delta\psi}\int_{\psi_1}^{\psi_2} \sin^2\mu d\psi}, \quad \Delta\psi \equiv \psi_2 - \psi_1 \tag{3.141}$$

From the foregoing definition, note that

$$0 < Q < 1 \tag{3.142}$$

Evaluating Q as given above is rather difficult because an expression for $\sin\mu$ is not readily derivable. However, an expression for $\cos\mu$ can be readily derived. Indeed, from Fig. 3.1 and the "cosine law", two expressions for $\overline{BD}^2$ can be derived:

$$\overline{BD}^2 = a_3^2 + a_4^2 - 2a_3a_4\cos\mu \tag{3.143a}$$
$$\overline{BD}^2 = a_1^2 + a_2^2 - 2a_1a_2\cos\psi \tag{3.143b}$$

Upon equating the two right-hand sides of the foregoing equations, an expression for $\cos\mu$ is derived in terms of the input angle, namely

$$\cos\mu = \frac{a_3^2 + a_4^2 - a_1^2 - a_2^2 + 2a_1a_2\cos\psi}{2a_3a_4} \tag{3.144}$$

If now relations (3.71) are recalled, an expression for $\cos\mu$ in terms of the linkage parameters $\{k_i\}_1^3$ is obtained:

$$\cos\mu = \mathrm{sgn}(k_2k_3)(c_1 + c_2\cos\psi) \tag{3.145a}$$

where coefficients c_1 and c_2 are defined as

$$c_1 \equiv \frac{k_2 - k_1k_3}{\sqrt{D}}, \quad c_2 = \frac{k_3^2}{\sqrt{D}} \tag{3.145b}$$

$$D \equiv k_2^2 + k_3^2 + k_2^2k_3^2 - 2k_1k_2k_3 \tag{3.145c}$$

Now the transmission quality Q can be written as $Q = \sqrt{1-\delta^2}$ where δ is the integral of $\cos^2\mu$ over the full mobility interval of the input link, i.e.,

$$\delta \equiv \sqrt{\frac{1}{\Delta\psi}\int_{\psi_1}^{\psi_2} \cos^2\mu d\psi}, \quad \Delta\psi \equiv \psi_2 - \psi_1 \tag{3.146}$$

and, by virtue of the relation between the transmission quality Q and δ, namely,

$$Q^2 + \delta^2 = 1 \tag{3.147}$$

it is reasonable to call δ the *transmission defect* of the linkage. Hence, maximizing Q is equivalent to minimizing δ. Note that δ^2 can be written as

$$\delta^2 \equiv \frac{1}{\Delta\psi}\left[c_1^2\Delta\psi + 2c_1c_2(\sin\psi_2 - \sin\psi_1) + \frac{1}{2}c_2^2\Delta\psi + \frac{c_2^2}{4}(\sin 2\psi_2 - \sin 2\psi_1)\right] \tag{3.148}$$

If, in particular, the input link is a crank, then,

$$\delta^2 = c_1^2 + \frac{1}{2}c_2^2 \tag{3.149}$$

In synthesizing a four-bar linkage for function generation, the location of the zeros of the dials of the ψ and ϕ values is normally immaterial. What matters is the *incremental values* of these angles from those zeros. We can thus introduce parameters α and β denoting the location of the zeros on the ψ and the ϕ dials, respectively, so that now

$$\psi_i = \alpha + \Delta\psi_i, \quad \phi_i = \beta + \Delta\phi_i, \quad \text{for} \quad i = 1, 2, \ldots, m \tag{3.150}$$

We can thus regard the least-square approximation $\mathbf{k}_0$ as a function of α and β, i.e.,

$$\mathbf{k}_0 = \mathbf{k}_0(\alpha, \beta) \tag{3.151}$$

It is apparent, then, that the two new parameters can be used to optimize the linkage performance, e.g., by minimizing its defect δ.

As it turns out, the transmission angle plays an important role not only in the force-transmission characteristics of the linkage, but also in the *sensitivity* of its positioning accuracy to changes in the nondimensional parameters $\mathbf{k}$. Indeed, if we make abstraction of the parameters α and β, for simplicity, we can calculate the sensitivity of the synthesized angle ϕ_i to changes in $\mathbf{k}$ from the input-output equation (3.11) written for the m prescribed input-output pairs. We display below the ith component of this vector equation:

$$F_i(\psi_i, \phi_i, \mathbf{k}) = k_1 + k_2 \cos\phi_i - k_3 \cos\psi_i - \cos(\psi_i - \phi_i) = 0, \; i = 1, 2, \ldots, m \qquad (3.152)$$

where ϕ_i is one of the two values of ϕ that verify the above equation for $\psi = \psi_i$, namely, the one lying closest to $\overline{\phi}_i$, as introduced in eq.(3.106). The sensitivity of interest is, apparently, $\partial\phi_i/\partial\mathbf{k}$, which is computed below:

$$\frac{\mathrm{d}F_i}{\mathrm{d}\mathbf{k}} = \frac{\partial F_i}{\partial\phi_i}\frac{\partial\phi_i}{\partial\mathbf{k}} + \frac{\partial F_i}{\partial\mathbf{k}} = \mathbf{0}$$

Hence,

$$\frac{\partial\phi_i}{\partial\mathbf{k}} = -\frac{\partial F_i/\partial\mathbf{k}}{\partial F_i/\partial\phi_i} \qquad (3.153)$$

Now, we calculate $\partial F_i/\partial\phi_i$ from eq.(3.152):

$$\frac{\partial F_i}{\partial\phi_i} = -k_2 \sin\phi - \sin(\psi_i - \phi_i) = -\frac{a_1 \sin\phi_i - a_2 \sin(\phi_i - \psi_i)}{a_2} \qquad (3.154)$$

A pertinent relation among the variables and parameters involved in eq.(3.154) is displayed in Fig. 3.17. From this figure,

$$a_1 \sin\phi_i - a_2 \sin(\phi_i - \psi_i) = a_3 \sin\mu_i \qquad (3.155)$$

Upon substitution of eq.(3.155) into eq.(3.154), we obtain

$$\frac{\partial F_i}{\partial\phi_i} = -\frac{a_3}{a_2}\sin\mu_i \qquad (3.156a)$$

which, when substituted into eq.(3.153), yields

$$\frac{\partial\phi_i}{\partial\mathbf{k}} = \frac{a_2}{a_3 \sin\mu_i}\frac{\partial F_i}{\partial\mathbf{k}} \qquad (3.156b)$$

Furthermore,

$$\frac{\partial F_i}{\partial\mathbf{k}} = \begin{bmatrix} 1 \\ \cos\phi_i \\ -\cos\psi_i \end{bmatrix} \qquad (3.156c)$$

and hence,

$$\frac{\partial\phi_i}{\partial\mathbf{k}} = \frac{a_2}{a_3 \sin\mu_i}\begin{bmatrix} 1 \\ \cos\phi_i \\ -\cos\psi_i \end{bmatrix} \qquad (3.156d)$$

It is now apparent that the larger $|\sin\mu_i|$, the less sensitive the positioning accuracy of the linkage is to changes in the linkage dimensions.

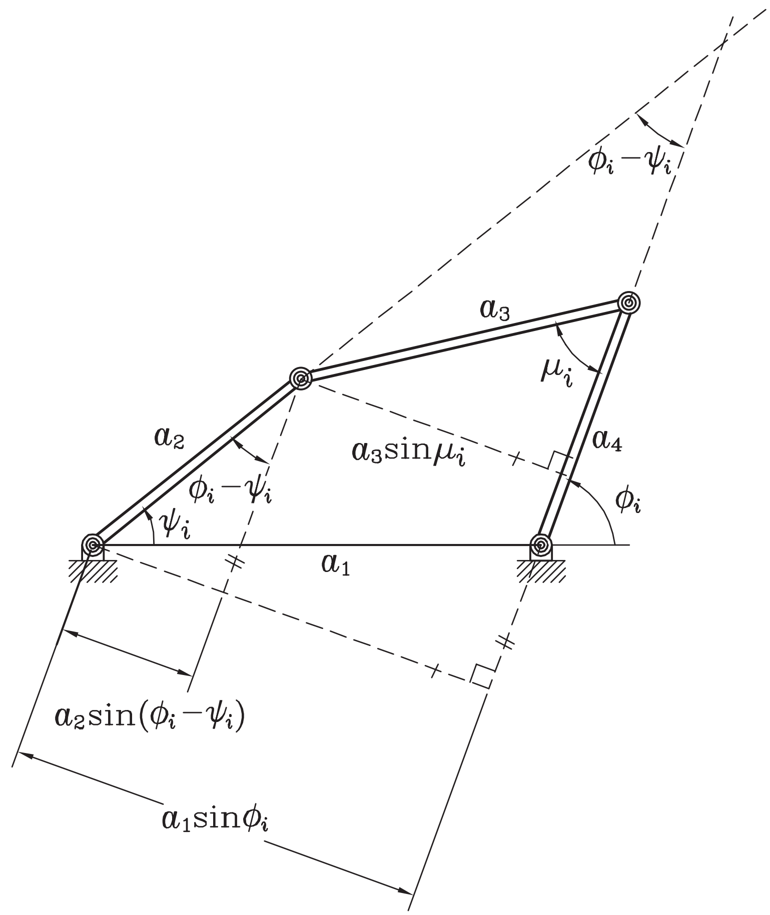

Figure 3.17: Relation between the transmission angle and the parameters and variables of a four-bar linkage

An interesting relation between the linkage discriminant defined in eq.(3.81a) and the transmission angle is now derived. From the expression for $\cos\mu$ obtained in eqs.(3.145a), an expression for $\sin^2\mu$ is readily obtained, in terms of the Freudenstein parameters, as

$$\sin^2\mu = \frac{k_3^2}{k_2^2 + k_3^2 + k_2^2 k_3^2 - 2k_1k_2k_3}\Delta(\psi) \tag{3.157a}$$

where $\Delta(\psi)$ is the linkage discriminant of eq.(3.81a), reproduced below for quick reference:

$$\Delta(\psi) \equiv -k_3^2\cos^2\psi + 2(k_1k_3 - k_2)\cos\psi + (1 - k_1^2 + k_2^2) \geq 0 \tag{3.157b}$$

which is nonnegative at feasible postures.

Apparently, then, for a given linkage, the square of the sine of the transmission angle is proportional to the discriminant. Hence, both vanish at dead points of the input link, which occur when this is a rocker.

3.6.2 Spherical Linkages: Transmission Angle and Transmission Quality

Spherical linkages are elusive to a kinetostatic analysis because they are *overconstrained spatial linkages,* in that the number of static equations available under the condition that all their axes intersect at one common point is smaller than the number of reaction forces and moments to be found. Rather than deriving the transmission angle for this kind of linkages by means of a kinetostatic analysis, as in the case of planar linkages, we derive it by establishing a correspondence between its geometry and that of the planar linkage. This is done by defining coordinate frames for the planar four-bar linkage in accordance with the Denavit-Hartenberg notation introduced in Subsection 3.2.2, with axes X_i, for $i = 1, \ldots, 4$ as illustrated in Fig. 3.18. Notice that axis Z_1 is defined in the foregoing figure as that of the output joint, passing through D, Z_2 as that of the input joint, passing through A, with similar definitions for axes Z_3 and Z_4, all these axes pointing outside of the plane of the figure, towards the reader.

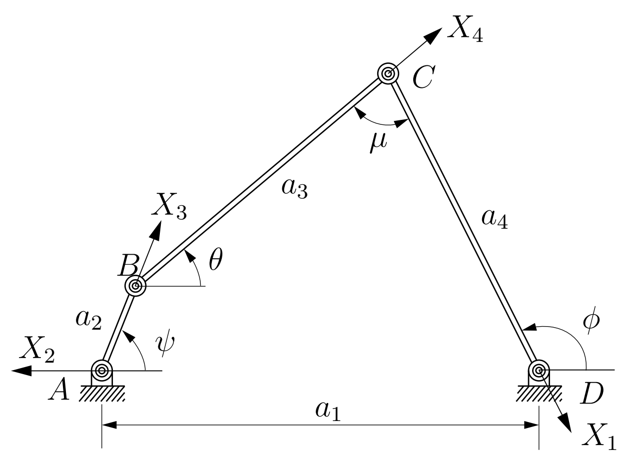

Figure 3.18: A four-bar linkage for function generation

It is now apparent that we can follow the Denavit-Hartenberg notation to define the transmission angle in this case as *the supplement* of that made by X_4 and X_1, positive in the direction of Z_4, which is θ_4 by definition. Indeed, as the reader can readily verify, based on the DH notation, $\theta_4 + \mu = \pi$ in the planar case. The same holds in the spherical case, and hence,

$$\cos\mu = -\cos\theta_4 \tag{3.158a}$$

An expression for $\cos\mu$ in terms of the input angle ψ can be found, as in the planar case, using trigonometry. Obviously, in the case at hand, spherical trigonometry is the tool to use, which then yields (McCarthy, 2000):

$$\cos\mu = \frac{c\alpha_3 c\alpha_4 - c\alpha_1 c\alpha_2 - s\alpha_1 s\alpha_2 \cos\psi}{s\alpha_3 s\alpha_4} \tag{3.158b}$$

The mechanical significance of the transmission angle is the same as in the planar case: the closer μ is to $\pm 90°$, the smaller the radial component of the force transmitted by the output link to the frame, and hence, the higher the quality of the force-transmission from the input to the output links. That is, for an acceptable performance, the dihedral angle between the planes of the circular arcs of the coupler and the output links should be such that the two planes are as far from each other as possible, which happens when the angle is $\pm 90°$, i.e., when $\cos\mu = 0$.

The transmission quality is defined exactly as in the planar case.

3.6.3 Spatial Linkages: Transmission Angle and Transmission Quality

This subsection is still under construction.

For quick reference, the spatial four-bar linkage of Fig. 3.5 is reproduced here as Fig. 3.19.

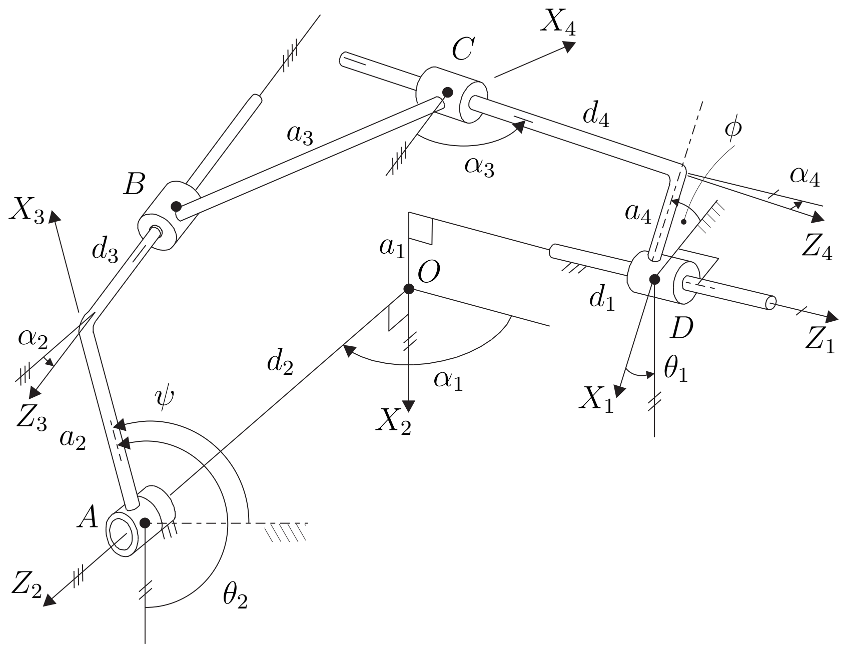

Figure 3.19: A RCCC linkage for function generation (Fig. 3.5 repeated)

Now, the simplest way of determining the transmission angle is by *dualization* of the expression in eq.(3.158a), namely, by putting hats on both μ and θ_4, which yields

$$\cos\hat{\mu} = -\cos\hat{\theta}_4 \tag{3.159a}$$

Similarly, an expression for $\cos\hat{\mu}$ in terms of the input angle ψ can be found upon *dualizing* both sides of eq.(3.158b), namely,

$$\cos\hat{\mu} = \frac{c\hat{\alpha}_3 c\hat{\alpha}_4 - c\hat{\alpha}_1 c\hat{\alpha}_2 - s\hat{\alpha}_1 s\hat{\alpha}_2 \cos\hat{\psi}}{s\hat{\alpha}_3 s\hat{\alpha}_4} \tag{3.159b}$$

In the foregoing equation, according with the definition of a dual angle given in eq.(A.5),

$$\hat{\mu} = \theta_4 + \epsilon d_4 \tag{3.160a}$$

where both are defined positive about and along the positive direction of Z_4. The geometric interpretation of the above expression is straightforward: while θ_4 is the angle between X_4 and X_1, d_4 is the signed distance between X_4 and X_1, the sign being determined by rule 5 of the DH notation. By the same token,

$$\hat{\alpha}_i = \alpha_i + \epsilon a_i \tag{3.160b}$$

which carries two constant quantities, while

$$\hat{\psi} = \psi + \epsilon d_1 \tag{3.160c}$$

carries one variable quantity, the input angle ψ, and a constant—usually positive, but not necessarily so—quantity with units of length, d_1. Moreover, the transmission quality is now a dual quantity, namely,

$$\hat{Q} \equiv \sqrt{\frac{1}{\Delta\psi}\int_{\psi_1}^{\psi_2} \sin^2\theta_4 d\psi} + \epsilon 2\sqrt{\frac{1}{\Delta\psi}\int_{\psi_1}^{\psi_2} d_4 \cos\theta_4 \sin\theta_4 d\psi}, \quad \Delta\psi \equiv \psi_2 - \psi_1 \tag{3.161}$$

Furthermore, θ_4 is the real angle between axes X_4 and X_1 in the spherical case, in which the two axes are concurrent. In the spatial case, $\hat{\theta}_4$ is the *dual angle* between two skew lines, axes X_4 and X_1. This angle, as discussed in Appendix A, comprises a primal part and a dual part, the former being the real angle between the two lines, as described above. The dual part is the signed distance between X_4 and X_1, which is positive when Z_4 points in the direction from X_4 to X_1. Thus, in the same way that the dot product of two unit vectors provides the cosine of the angle between the two vectors, the dot product of two *dual unit vectors*—a dual vector is "of unit magnitude" when its primal part is a real unit vector—provides the cosine of the (dual) angle between two lines. The dual angle in question involves both the angle between the two lines and their signed distance.

In the planar case, $\cos\mu$ determines "how far" the axis of the coupler link is from the output link, while keeping one common point, C, at any linkage posture. In the spherical case, $\cos\mu$ determines "how far" the plane of the circular arc of the coupler link is from the counterpart circular arc of the output link, while maintaining one common line, Z_4, at any given linkage posture.

The generalization to the spatial case then follows: $\cos\hat{\mu}$ determines "how far" X_4, while intersecting Z_4, is from X_1 at any given linkage posture. When the two axes coincide, the worst-case scenario, the full *wrench*—force and moment—transmitted by the coupler link to the output link goes into the linkage support, and no part of it is used to counter the load applied on the output link. The effect of the transmitted force on the output link is the same as that of a force applied to a door along a line of action that passes through the hinge axis and a moment lying in a plane normal to this axis. Force and moment, in this case, are incapable of turning the door.

In summary, then, minimizing the dual transmission quality of the spatial four-bar linkage is equivalent to keeping the axis of the coupler link as "far away" as possible from axis X_1 of the DH notation.

Exercise 3.6.1 Under static, conservative conditions, show that the line of action of the force transmitted by the coupler link to the output link is X_4.

Exercise 3.6.2 Derive the expression for the dual transmission quality given in eq.(3.161), then specialize it for the case of an input crank.

3.7 Design Error vs. Structural Error

In this section we establish the relation between the design error and the structural error. In doing this, we build upon the analysis proposed by Tinubu and Gupta (1984).

The structural error was introduced in eq.(3.106). If now $\boldsymbol{\phi}$ and $\overline{\boldsymbol{\phi}}$ denote the m-dimensional vectors of *generated and prescribed output values*, then the structural-error vector $\mathbf{s}$ can be expressed as

$$\mathbf{s} \equiv \boldsymbol{\phi} - \overline{\boldsymbol{\phi}} \tag{3.162}$$

where, it is recalled, ϕ_i denotes the *generated* value, $\overline{\phi}_i$ the *prescribed* value of the output angle for a given value ψ_i of the input angle. In the ensuing discussion we assume that the synthesis equations are cast in the general form

$$\mathbf{S}\mathbf{k} = \mathbf{b} \tag{3.163}$$

regardless of the type of linkage, planar, spherical or spatial. However, one should keep in mind that, in the spatial case, $\mathbf{S}$, $\mathbf{b}$ and $\mathbf{k}$ become all dual quantities: $\hat{\mathbf{S}}$, $\hat{\mathbf{b}}$ and $\hat{\mathbf{k}}$. In this context, $\mathbf{S}$ is a $m \times n$ matrix, while $\mathbf{k}$ and $\mathbf{b}$ are n- and m-dimensional vectors, respectively. Obviously, $n = 3,\ 4$ or 8, depending on the type of linkage, planar, spherical or spatial[10]. In the case of spatial linkages, a second equation of the same gestalt as that of eq.(3.163), involving a second vector of Freudenstein parameters—the dual part of the dual vector $\hat{\mathbf{k}}$—occurs, as per eqs.(3.120a & b).The difference $\mathbf{e} \equiv \mathbf{b} - \mathbf{S}\mathbf{k}$—or its dual counterpart for that matter—is to be highlighted: minimizing a norm of $\mathbf{e}$ is not equivalent to minimizing the same norm of $\mathbf{s}$. Indeed, while $\mathbf{e}$ denotes the error in meeting the synthesis equations, whose components involve trigonometric functions of the input and output angles at the m prescribed pairs, $\mathbf{s}$ denotes the error in meeting the prescribed positions, which is what really matters. Unfortunately, however, a relation of the form $\mathbf{g} \equiv \mathbf{g}(\mathbf{e}, \mathbf{s}) = \mathbf{0}$ between

[10]See footnote 5 of this chapter.

the two errors is elusive. Nevertheless, a *differential* relation between the two errors can be readily obtained, as done below, and that suffices.

In minimizing the structural error, we aim at a minimum of the rms value of the components of vector $\mathbf{s}$ by properly choosing $\mathbf{k}$:

$$z(\mathbf{k}) \equiv \frac{1}{2m}\|\mathbf{s}\|^2 \quad \rightarrow \quad \min_{\mathbf{k}} \tag{3.164}$$

where $\|\mathbf{s}\|$ is the Euclidean norm of the structural error $\mathbf{s}$.

Function $z(\mathbf{k})$ attains a *stationary* value with respect to $\mathbf{k}$ when its *gradient* vanishes, i.e.,

$$\nabla z \equiv \frac{\partial z}{\partial \mathbf{k}} = \left(\frac{\partial \mathbf{s}}{\partial \mathbf{k}}\right)^T \frac{\partial z}{\partial \mathbf{s}} = \mathbf{0}_n \tag{3.165}$$

with $\mathbf{0}_n$ denoting the n-dimensional zero vector. The above equation is the *normality condition* of the minimization problem at hand. Apparently,

$$\frac{\partial z}{\partial \mathbf{s}} = \frac{1}{m}\mathbf{s} \tag{3.166}$$

Now, in order to compute $\partial\mathbf{s}/\partial\mathbf{k}$, we recall the definition of $\mathbf{s}$, eq.(3.162), which leads to

$$\frac{\partial \mathbf{s}}{\partial \mathbf{k}} = \frac{\partial \boldsymbol{\phi}}{\partial \mathbf{k}} \tag{3.167}$$

as $\overline{\boldsymbol{\phi}}$ is a constant vector of prescribed output values. Moreover, the ith row of matrix $\partial\boldsymbol{\phi}/\partial\mathbf{k}$, for the *planar case*, is displayed in eq.(3.156d) as a column array.

Now, in order to compute $\partial\boldsymbol{\phi}/\partial\mathbf{k}$, we need an equation relating the array $\boldsymbol{\phi}$ of *generated values* of the output angle with vector $\mathbf{k}$. One candidate would be the m synthesis equations (3.163), which define the *design error* $\mathbf{e}$:

$$\mathbf{e} \equiv \mathbf{e}(\boldsymbol{\phi},\, \mathbf{k}) = \mathbf{b} - \mathbf{S}\mathbf{k} \tag{3.168}$$

The above expression is, in general, different from zero, when evaluated at the *prescribed* values $\overline{\phi}_i$ of the output angle, for $i = 1, \ldots, m$, and hence, does not define an implicit equation in $\boldsymbol{\phi}$ and $\mathbf{k}$. As a matter of fact, the problem of approximate synthesis consists in minimizing the Euclidean norm of the nonzero vector $\mathbf{e}$.

However, when the above vector is evaluated at the *generated* values ϕ_i of the output angle, for $i = 1, \ldots, m$, then it does vanish. Indeed, the ith component of $\mathbf{e}$ as defined in eq.(3.168) is nothing but the input-output function $F(\psi, \phi) = 0$ evaluated at ψ_i for a given linkage defined by $\mathbf{k}$. In our case, $\mathbf{k}$ is the *current value*, within an iterative process, to be formulated in Subsection 3.7.1, of the unknown vector of linkage parameters, i.e., the Freudenstein parameters. Upon solving the input-output equation for ϕ, two values of ϕ_i are obtained, as found in Section 3.4, and hence, the function does vanish at these two values. We will assume that, of these two values, ϕ_i is chosen as the one closer to $\overline{\phi}_i$. We thus have

$$F(\psi_i, \phi_i) \equiv b_i - \mathbf{s}_i^T\mathbf{k} = 0 \tag{3.169}$$

in which $\mathbf{s}_i^T$ denotes the ith row of $\mathbf{S}$ and b_i the ith component of $\mathbf{b}$.

To avoid confusion, let us distinguish between the design error $\mathbf{e}$ when evaluated at $\boldsymbol{\phi}$ and when evaluated at $\overline{\boldsymbol{\phi}}$, by denoting the latter by $\overline{\mathbf{e}}$, i.e.,

$$\overline{\mathbf{e}} \equiv \mathbf{e}(\overline{\boldsymbol{\phi}}, \mathbf{k}) = \overline{\mathbf{b}} - \overline{\mathbf{S}}\mathbf{k} \neq \mathbf{0} \tag{3.170}$$

where $\overline{\mathbf{S}}$ and $\overline{\mathbf{b}}$ denote $\mathbf{S}$ and $\mathbf{b}$, respectively, when evaluated at the prescribed values of the input angle $\{\,\psi_i\,\}_1^m$ and at the generated $\overline{\boldsymbol{\phi}}$.

Moreover, when we evaluate $\mathbf{e}$ at the *generated* value $\boldsymbol{\phi}$, we obtain

$$\mathbf{e} \equiv \mathbf{e}(\boldsymbol{\phi}, \mathbf{k}) = \mathbf{b} - \mathbf{S}\mathbf{k} = \mathbf{0}_m \tag{3.171}$$

which is an *implicit* vector function of $\boldsymbol{\phi}$ and $\mathbf{k}$, and hence, allows for the evaluation of $\partial\boldsymbol{\phi}/\partial\mathbf{k}$. Upon differentiation of eq.(3.171) with respect to $\mathbf{k}$, we obtain

$$\frac{\mathrm{d}\mathbf{e}}{\mathrm{d}\mathbf{k}} = \frac{\partial\mathbf{e}}{\partial\mathbf{k}} + \frac{\partial\mathbf{e}}{\partial\boldsymbol{\phi}}\frac{\partial\boldsymbol{\phi}}{\partial\mathbf{k}} = \mathbf{O}_{mn} \tag{3.172}$$

where $\mathbf{O}_{mn}$ is the $m \times n$ zero matrix. Moreover, the $m \times m$ matrix $\partial\mathbf{e}/\partial\boldsymbol{\phi}$ is computed from the input-output equation (3.169), or its dual counterpart, as the case may be. Since e_k is influenced only by ϕ_k, and not by ϕ_j, for $j \neq k$, $\partial\mathbf{e}/\partial\boldsymbol{\phi}$ is diagonal, i.e.,

$$\frac{\partial\mathbf{e}}{\partial\boldsymbol{\phi}} = \mathrm{diag}\,[\,\partial e_1/\partial\phi_1 \quad \partial e_2/\partial\phi_2 \quad \cdots \quad \partial e_m/\partial\phi_m\,] \equiv \mathbf{D} \tag{3.173a}$$

Under the assumption that none of the diagonal elements of $\mathbf{D}$ vanishes, this matrix is nonsingular, and hence, the matrix $\partial\boldsymbol{\phi}/\partial\mathbf{k}$ sought can be solved for from eq.(3.172). Furthermore, it is apparent from eq.(3.171) that $\partial\mathbf{e}/\partial\mathbf{k}$ is nothing but the negative of the synthesis matrix $\mathbf{S}$, evaluated at the generated values of the output angle, i.e.,

$$\frac{\partial\mathbf{e}}{\partial\mathbf{k}} = -\mathbf{S} \tag{3.173b}$$

Hence, $\partial\boldsymbol{\phi}/\partial\mathbf{k}$, as computed from eq.(3.172), is

$$\frac{\partial\boldsymbol{\phi}}{\partial\mathbf{k}} \equiv \frac{\partial\mathbf{s}}{\partial\mathbf{k}} = \mathbf{D}^{-1}\mathbf{S} \tag{3.174}$$

Therefore, the normality condition (3.165) leads to

$$\mathbf{S}^T\mathbf{D}^{-1}\mathbf{s} = \mathbf{0}_n \tag{3.175}$$

where $\mathbf{0}_n$ denotes the n-dimensional zero vector. The normality condition thus states that, for $\mathbf{k}$ to produce a stationary value of the positioning error—proportional to the rms value of the structural error $\mathbf{s}$—the structural error $\mathbf{s}$ must lie in the null space of the matrix product $\mathbf{S}^T\mathbf{D}^{-1}$. That is, the structural error of minimum norm need not vanish and, in general, it won't, but must verify eq.(3.175).

Now, contrary to the minimization of the design error, the minimization of the positioning error leads to a *nonlinear least-square problem*, which must be solved *iteratively*, as described in Subsection 3.7.1.

3.7.1 Minimizing the Structural Error

The approach followed here is similar to the Newton-Gauss method used to solve nonlinear least-square problems, as outlined in Subsection 1.6.1: for starters, a sequence $\mathbf{s}^0$, $\mathbf{s}^1$, ..., $\mathbf{s}^i$, $\mathbf{s}^{i+1}$ of structural-error vector values is generated, which, upon convergence, should verify the normality condition. For a given $\mathbf{s}^i$, an improved vector value $\mathbf{s}^{i+1}$ is obtained from the *first-order approximation* of $\mathbf{s}$:

$$\mathbf{s}^{i+1} \approx \mathbf{s}^i + \left.\frac{\partial \mathbf{s}}{\partial \mathbf{k}}\right|_{\mathbf{k}=\mathbf{k}^i} \Delta\mathbf{k}^i = \mathbf{s}^i + \mathbf{D}_i^{-1}\mathbf{S}_i\Delta\mathbf{k}^i \tag{3.176}$$

where $\mathbf{D}_i \equiv \mathbf{D}|_{\mathbf{k}=\mathbf{k}^i}$ and $\mathbf{S}_i \equiv \mathbf{S}|_{\mathbf{k}=\mathbf{k}^i}$. Hence,

$$\mathbf{D}_i^{-1}\mathbf{S}_i\Delta\mathbf{k}^i = \mathbf{s}^{i+1} - \mathbf{s}^i \tag{3.177}$$

Upon solving for $\Delta\mathbf{k}^i$, the above equation allows the updating of $\mathbf{k}$ as $\mathbf{k}^{i+1} = \mathbf{k}^i + \Delta\mathbf{k}^i$. However, in eq.(3.177) we don't know $\mathbf{s}^{i+1}$. Moreover, upon convergence, $\mathbf{s}$ needn't vanish, and most likely it won't. We can thus assume that $\mathbf{s}^{i+1} \neq \mathbf{0}_m$, but, if $\mathbf{k}^{i+1}$ is an improvement over $\mathbf{k}^i$, then the corresponding structural error $\mathbf{s}^{i+1}$ will be "close" to verifying the normality condition (3.175). In fact, let us assume that $\mathbf{s}^{i+1}$ does verify the normality condition, with $\mathbf{S}$ and $\mathbf{D}$ evaluated at $\mathbf{k} = \mathbf{k}^i$, as we cannot evaluate them at $\mathbf{k}^{i+1}$. Further, let us multiply both sides of eq.(3.177) from the left by $\mathbf{S}_i^T\mathbf{D}_i^{-1}$, which yields

$$\mathbf{S}_i^T\mathbf{D}_i^{-1}\mathbf{D}_i^{-1}\mathbf{S}_i\Delta\mathbf{k}^i = -\mathbf{S}_i^T\mathbf{D}_i^{-1}\mathbf{s}^i \tag{3.178}$$

where the term linear in $\mathbf{s}^{i+1}$ has dropped because it has been assumed to verify the normality conditions. In eq.(3.178) the coefficient of $\Delta\mathbf{k}^i$ is a square $n \times n$ matrix—with n being the dimension of vector $\mathbf{k}$—which allows for the computation of $\Delta\mathbf{k}^i$ in the form

$$\Delta\mathbf{k}^i = -(\mathbf{S}_i^T\mathbf{D}_i^{-2}\mathbf{S}_i)^{-1}\mathbf{S}_i^T\mathbf{D}_i^{-1}\mathbf{s}^i \tag{3.179}$$

thereby showing that the correction $\Delta\mathbf{k}^i$ can be computed with the numerical values available at the ith iteration. In fact, the expression for $\Delta\mathbf{k}^i$ given in eq.(3.179) should be regarded as a *formula*, not as an algorithm. Indeed, the verbatim inversion of the matrix in parentheses in the foregoing equation is *to be avoided* due to its high *condition number*[11]. As a matter of fact, the condition number, in either the Euclidean or the Frobenius norm, of the same $n \times n$ matrix is exactly the square of the same norm of the $m \times n$ matrix $\mathbf{D}_i^{-1}\mathbf{S}_i$. Hence, a formulation is sought that will allow the computation of $\Delta\mathbf{k}^i$ from a system of equations involving the foregoing rectangular matrix. If we recall Subsection 1.4.5, the right-hand side of eq.(3.179) is the *least-square approximation* of the *overdetermined system*

$$(\mathbf{D}_i^{-1}\mathbf{S}_i)\Delta\mathbf{k}^i = -\mathbf{s}^i \tag{3.180}$$

[11]See the definition of this concept in Section 1.4.4.

which is identical to eq.(3.177) when the therm $\mathbf{s}^{i+1}$ is dropped. Notice, however, that this term couldn't simply be dropped from the above-mentioned equation on the basis that the said term vanishes, because the structural error is not expected to vanish at the optimum solution. The computation of $\Delta\mathbf{k}^i$ from eq.(3.180) now should be pursued via an orthogonalization procedure, as studied in Subsection 1.4.5. With $\Delta\mathbf{k}^i$ calculated, the ith iteration is complete, as a new, improved value $\mathbf{k}^{i+1}$ of the design parameter vector $\mathbf{k}$ is available. Now the new structural-error vector value $\mathbf{s}^{i+1}$ can be computed, and then the normality condition verified. If the condition is not verified, a new iteration is in order; if the same condition is verified, then the procedure stops. An alternative convergence criterion, equivalent to the latter, is to verify whether $\|\Delta\mathbf{k}^i\| < \epsilon$, for a prescribed tolerance ϵ. The equivalence of the two criteria should be apparent from the relation between $\Delta\mathbf{k}^i$ and the product of the last three factors of the right-hand side of eq.(3.179).

Branch-switching Detection

This Subsubsection is limited to planar linkages, its generalization to spherical and spatial linkages should be doable, as the problem under study is based on the concept of the sign of the transmission index. The latter was studied in Section 3.6.

In the foregoing analysis an implicit assumption was adopted: all generated values $\{\,\phi_i\,\}_1^m$ lie on the same linkage branch. However, all four-bar linkages studied in this chapter, planar, spherical and spatial, were shown in Section 3.4 to be *bimodal*, i.e., they all entail two solution branches of their input-output equation. This means that, within an iteration loop, the occurrence of branch-switching should be monitored. Below we explain a simple means of doing this, as applicable to planar linkages. The two branches of a typical planar four-bar linkage are apparent in Fig. 3.8(a). In this figure, the transmission angle is $\mu = \angle BCD$ in one branch, in the second being $\mu' = \angle BC'D$. The qualitative difference between the two branches lies in *the sign of the sine of the transmission angle*, for, in the first branch, we have $\sin\mu > 0$; in the second, $\sin\mu' < 0$. Moreover, $\sin\mu$ vanishes at *deadpoints*, when the input angle reaches either a maximum or a minimum—linkages of this kind have an input rocker. Hence, a simple way of deciding whether all values $\{\,\phi_i\,\}_1^m$ lie in the same branch relies on the computation of $\sin\mu$ with the correct sign. This is most simply done by means of the 2D version of the cross product[12] of vectors $\overrightarrow{CB} = \mathbf{b} - \mathbf{c}$ and $\overrightarrow{CD} = \mathbf{d} - \mathbf{c}$, in this order, where $\mathbf{b}$, $\mathbf{c}$ and $\mathbf{d}$ are the position vectors of points B, C and D, respectively, in the given coordinate frame. The product at stake is given by

$$p \equiv (\mathbf{b} - \mathbf{c})^T\mathbf{E}(\mathbf{d} - \mathbf{c}) = \|\mathbf{b} - \mathbf{c}\|\|\mathbf{d} - \mathbf{c}\|\sin\mu = a_3a_4\sin\mu \qquad (3.181)$$

[12]See Subsection 1.4.1.

with $\mathbf{E}$ introduced in eq.(1.1a). Given that the link lengths are positive, we have the relation

$$\mathrm{sgn}(\sin\mu) = \mathrm{sgn}(p) \tag{3.182}$$

which now can be used to monitor branch-switching.

Introducing a Massive Number of Data Points

As shown by Hayes et al. (1999), one simple way of minimizing the structural error is via design-error minimization *in the presence of a large number of prescribed poses.* We show with one example below that, as the cardinality m of the data set increases, the design and structural errors converge. The results are taken from the foregoing reference.

In the example below, the *weighted Euclidean norm* of the design and the structural error, $\|\mathbf{e}\|_{2W}$ and $\|\mathbf{s}\|_{2W}$, respectively, are minimized. For any m-dimensional vector $\mathbf{v}$, this norm is defined as the rms value of its components, namely,

$$\|\mathbf{v}\|_{2W} \equiv \sqrt{\frac{1}{m}\mathbf{v}^T\mathbf{v}} \tag{3.183}$$

Example 3.7.1 *We synthesize here a planar and a spherical* RRRR *four-bar linkage to generate a quadratic I/O function for the values given below:*

$$\psi_i = \alpha + \Delta\psi_i,\ \phi_i = \beta + \Delta\phi_i,\ \Delta\phi_i = \frac{9\Delta\psi_i^2}{8\pi},\ i = 1, \ldots, m$$

For each linkage the I/O dial zeros (α and β) are selected to minimize the condition number κ of $\mathbf{S}$ for each data-set, in following the procedure proposed by Liu and Angeles (1993). Then both the design and structural errors are determined for the linkages that minimize the respective Euclidean norms for data-sets with cardinalities of $m = \{10, 40, 70, \text{ and } 100\}$*. These results are listed in Tables 3.5–3.8. Finally the structural errors, corresponding to $m = 40$, of the linkages that minimize the Euclidean norms of the design and structural errors are graphically displayed in Fig. 3.20.*

Table 3.5: Results for $m = 10$.

	Planar RRRR	Spherical RRRR
α_{opt} (°)	123.8668	43.3182
β_{opt} (°)	91.7157	89.5221
κ_{opt}	33.2974	200.5262
$\|\mathbf{d}\|_{2W}$	2.2999×10^{-3}	2.4033×10^{-4}
$\|\mathbf{s}\|_{2W}$	1.8863×10^{-3}	1.3187×10^{-4}

Table 3.6: Results for $m = 40$.

	Planar RRRR	Spherical RRRR
α_{opt} ($^\circ$)	117.4593	42.7696
β_{opt} ($^\circ$)	89.4020	88.8964
κ_{opt}	32.5549	203.0317
$\|\mathbf{d}\|_{2W}$	2.484×10^{-3}	2.984×10^{-4}
$\|\mathbf{s}\|_{2W}$	2.375×10^{-3}	1.671×10^{-4}

Table 3.7: Results for $m = 70$.

	Planar RRRR	Spherical RRRR
α_{opt} ($^\circ$)	116.4699	42.7014
β_{opt} ($^\circ$)	89.0488	88.8045
κ_{opt}	32.5242	204.7696
$\|\mathbf{d}\|_{2W}$	2.496×10^{-3}	3.031×10^{-4}
$\|\mathbf{s}\|_{2W}$	2.438×10^{-3}	1.701×10^{-4}

3.8 Synthesis Under Mobility Constraints

Read (Liu and Angeles, 1992).

3.9 Synthesis of Complex Linkages

To come.

3.9.1 Synthesis of Stephenson Linkages

To come.

Table 3.8: Results for $m = 100$.

	Planar RRRR	Spherical RRRR
α_{opt} ($^\circ$)	116.0679	42.6740
β_{opt} ($^\circ$)	88.9057	88.7674
κ_{opt}	32.5170	205.5603
$\|\mathbf{d}\|_{2W}$	2.499×10^{-3}	3.047×10^{-4}
$\|\mathbf{s}\|_{2W}$	2.464×10^{-3}	1.712×10^{-4}

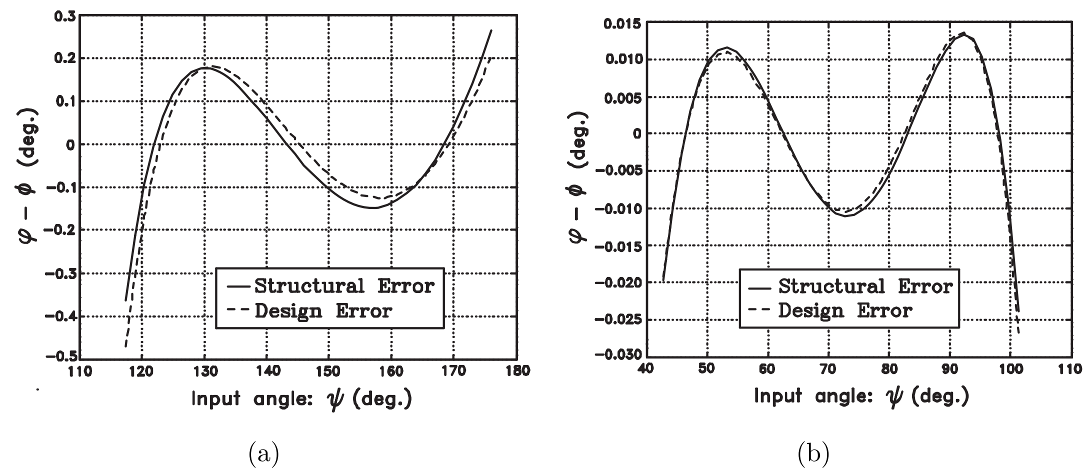

Figure 3.20: Structural error comparison for: (a) planar and (b) spherical RRRR linkages upon minimizing $\|\mathbf{s}\|_{2W}$ & $\|\mathbf{e}\|_{2W}$.